

Electronic Supplementary Information

Recyclable, Reprocessable, Self-adhered and Repairable Carbon Fiber Reinforced Polymers Using Full Biobased Matrices from Camphoric Acid and Epoxidized Soybean Oil

*Weiwei Zhang,^{‡a,b} Jianqiao Wu,^{‡b} Liang Gao,^c Baoyan Zhang,^c Jianxin Jiang^{*a} and Jun Hu^{*b}*

^a Department of Chemistry and Chemical Engineering, MOE Engineering Research Center of Forestry Biomass Materials and Bioenergy, National Forest and Grass Administration Woody Spices (East China) Engineering Technology Research Center, Beijing Forestry University, Beijing 100083, China.

^b Beijing Advanced Innovation Center for Soft Matter Science and Engineering, Beijing University of Chemical Technology, Beijing 100029, China.

^c Department of Resin & Prepreg, AVIC Manufacturing Technology Institute Composite Technology Center, Beijing 101300, China.

[‡] These authors contributed equally to this work.

*Corresponding Authors

Email: jiangjx@bjfu.edu.cn, jhu@mail.buct.edu.cn

The supporting information includes 19 pages, 15 figures, 1 table and 1 scheme.

Contents

S1. Experimental section	Page S3
S2. DSC analysis for CPA, ESO, and CPA/ESO without TBD.....	Page S8
S3. FTIR spectra of ESO, CPA and CPA/ESO networks	Page S9
S4. Reaction mechanism of ESO with CPA	Page S9
S5. DTG of CPA/ESO networks.....	Page S10
S6. Hydrolysis resistance of CPA/ESO (R = 1.25)	Page S10
S7. Stress relaxation of CPA/ESO networks.....	Page S11
S8. Calculation of T_v of CPA/ESO (R = 1.25)	Page S11
S9. Digital photo, flexural tests and DMA of CF/CPA/ESO composites.	Page S13
S10. Compression performance tests for reprocessed CF/CPA/ESO composite “M” and CPA/ESO (R = 1.25) matrices.	Page S15
S11. Repairing properties of CF/CPA/ESO composites at 200°C without EG	Page S16
S12. Degradation kinetics of pure matrices (CPA/ESO, R = 1.25) in EG at 190°C.	Page S17
S13. Comparison of the matrices in this work with other reported dynamic matrices for fiber reinforced polymers.....	Page S18
References.....	Page S19

S1. Experimental section

Differential scanning calorimeter (DSC, TA-Q20) was used to investigate the exothermic process during curing. The samples (5 mg) were sealed in aluminum crucibles, and scanned at a heating rate of 5°C/min for curing samples and raw materials.

Fourier transform infrared spectroscopy (FTIR) were conducted on a spectrophotometer (Nicolet iS5). The sample was grinded with potassium bromide (KBr, 100 mg) in a mortar, and the mixture was compressed into a disk using a mould. All samples were scanned from 4000 to 400 cm⁻¹.

Thermal stability test: Thermal stability was measured using a thermogravimetric analyzer (TGA, TA-Q50). Samples (~5 mg) were loaded into alumina crucibles and scanned from 30 to 700 °C at a heating rate of 10 °C/min under nitrogen atmosphere.

Gel content tests: The dry sample (30 mg, m_0) was immersed in 5 mL acetonitrile for 20 h. After 20 h, the samples were dried in a vacuum oven at 60°C for 10 h and then weighted (m_1). The gel content was calculated according to the following equation:

$$\text{Gel contents (\%)} = \frac{m_1}{m_0} \times 100\% \quad (\text{S1})$$

Swelling tests: The swelling ratio was measured by immersing the sample (~30 mg, m_0) in acetonitrile at room temperature. When the absorption reached equilibrium, the sample was taken out of the solution. The excessive surface solvent was removed with a filter paper, and the swollen sample was weighted (m_1). The swelling ratio was calculated according to the following equation:

$$\text{Swelling ratio (\%)} = \frac{m_1 - m_0}{m_0} \times 100\% \quad (\text{S2})$$

Hydrolysis resistance tests: The dry sample (30 mg) was initially immersed in 10 mL H₂O, and then was set in a vacuum oven at 80°C. The sample was taken out of the water at different hydrolysis time, the excessive surface solvent was removed with a filter paper, and the swollen sample was weighted. After drying in a vacuum oven at 100°C for 10 h, the sample was measured. The gel content and swelling ratio were calculated according to the equation S1 and S2, respectively.

Dynamic mechanical analysis: Dynamic mechanical properties were measured using a dynamic mechanical analyzer (DMA, TA-Q850). For CPA/ESO matrices, the sample with a dimension of 30 mm × 5 mm × 1 mm was scanned from -30 to 100°C at a heating rate of 5°C/min in tension mode. For CF/CPA/ESO composites, the sample with a dimension of 60 mm × 10 mm × 1 mm was scanned from 20 to 200°C at a heating rate of 5°C/min by using double-cantilever mode. The amplitude was set at 10 μm and the frequency was 1 Hz.

Tensile tests for CPA/ESO matrices: The tensile strength and modulus were measured on an Instron 5565A instrument at room temperature. Dumbbell specimens used for the measurement were prepared by tailoring the sample sheets with a dumbbell-shaped cutter. The width and thickness of the specimens were 4 mm and 1 mm, respectively. A stretching speed of 5 mm/min was employed during the measurement. At least five samples were tested for all the samples.

Stress relaxation test: Stress relaxation experiment was performed on a TA-ARG2 rheometer using the 8 mm parallel-plate geometry. The sample was heated to appointed temperature and soaked for 3 min with a constant 1% strain and normal force of 10 N.

Welding, repairing, physical recycling tests for CPA/ESO matrices: Welding property was studied using an oven at 200°C. Three pieces were assembled into an “N” pattern without any

pressure at 200°C for 60 min. Repairing property was studied using an optical microscope (UPT200I). The sample was cracked using a knife and repaired at an oven at 200°C. A glass slide was added on the sample to offer a small pressure. Physical recycling properties were studied by using tensile test similar with the original samples. The films were cut into small pieces and put into mold on a press vulcanizer at 200 °C for 1 h at 10 tons pressure to form recycled samples.

X-ray 3D microscope observation for CF/CPA/ESO composites: The X-ray 3D microscope (nano Voxe 12000) was used to observe the inside structures of CF/CPA/ESO composites. The sample with a dimension of 10 mm × 10 mm × 1 mm was used for the tests. The images and the movie of XZ, XY and YZ cross profile were obtained. The tests were offered by AVIC Composite Co., LTD Composite Testing Technology Center.

Tensile and flexural tests for CF/CPA/ESO composites: The tensile and flexural tests were measured on an Electromechanical universal testing machine (ETM504C, Hubei Wance Test Machine Co. Ltd., China) at room temperature. The samples with a dimension of 60 mm × 15 mm × 1 mm were used for the test. A stretching speed of 5 mm/min was employed during the measurement. At least five samples were tested for all the samples.

Reprocessing tests for CF/CPA/ESO composites: A 40 mm × 10 mm × 1 mm CF/CPA/ESO composites sheet was placed inside preheated zigzag mold and reprocessed on a press vulcanizer at 200°C for 0.5 h at 5 tons pressure. After cooling to room temperature, a zigzag shaped 3D composite was obtained.

Compression tests for CF/CPA/ESO composites and CPA/ESO matrices: The compression tests for CF/CPA/ESO composites were performed using an electromechanical universal testing machine (ETM504C, Hubei Wance Test Machine Co. Ltd., China). A compressing speed of 2

mm/min was employed during the measurement. The compression tests for CPA/ESO matrices were performed using the same machine. A 10 mm × 10 mm × 15 mm CPA/ESO sample was prepared using the same curing process in an oven. The compressing and recovering speed of 2 mm/min were employed during the measurement.

Self-adhering tests for CF/CPA/ESO composites: The CF/CPA/ESO composites were 60 mm × 10 mm × 1 mm with the overlap area was 15 mm × 1 mm, and welding at an oven at 200°C. A clip was added on the sample to offer a small pressure. After 60 min, the welded samples were used for lap-shear measurements using an Electromechanical universal testing machine (ETM504C, Hubei Wance Test Machine Co. Ltd., China). A stretching speed of 5 mm/min was employed during the measurement. At least five samples were tested for all the samples.

Repairing tests of CF/CPA/ESO composites: Repairing property was studied using an optical microscope (UPT200I). The sample was cracked using a knife, then added a drop of ethylene glycol to the crack and repaired at an oven at 200°C. A glass slide was added on the sample to offer a small pressure. According to the above process, another sample was performed without the addition of EG.

Degradation of pure matrices and CF/CPA/ESO composites: Pure matrices (~30 mg) and CF/CPA/ESO composite laminates (~50 mg) were placed in ethylene glycol (EG, 5 mL for each sample) at 190°C, respectively. The sample was taken out of EG at different degradation time and then dried at 200°C for 24 h. At least three repeats were performed at each time. The cleavage planes of CF/CPA/ESO composites during degradation process were observed using scanning electron microscope (SEM, SU8010, Japan) with an accelerating potential of 5 kV. For samples at

2 h, 10 h and 20 h, these composites from EG were dried at 200°C for 24 h and cleaved without washing.

Fiber recycling of CF/CPA/ESO composites: A CF/ESO/CPA composite laminate with dimensions of 30 mm × 6 mm × 1 mm was placed in 15 mL ethylene glycol at 190°C in a high pressure reactor. After the epoxy resin was completely degraded, the CF was washed with acetone and then dried at 50°C for 24 h.

Characterization of virgin CF and recycled CF: The morphologies of virgin CF and recycled CF were observed using a scanning electron microscope (SEM, SU8010, Japan) with an accelerating potential of 5 kV. Raman spectra of virgin CF and recycled CF were measured using an inVia-Reflex Raman spectrometer, 60 s exposure time and 12 mW laser energy. The tensile test of CF monofilaments was conducted on a XQ-2 single fibre tester with a gauge length of 20 mm at a crosshead speed of 5 mm/min at room temperature. The tensile test of CF monofilaments were randomly selected from CF cloths and at least 10 specimens were successfully tested for each group.

S2. DSC analysis for CPA, ESO, and CPA/ESO without TBD

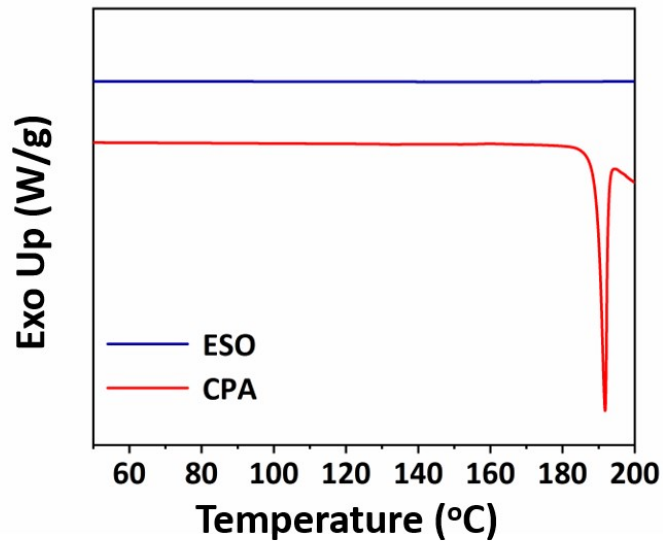


Fig.S1 DSC curves of ESO and CPA at a heating rate of 5°C/min.

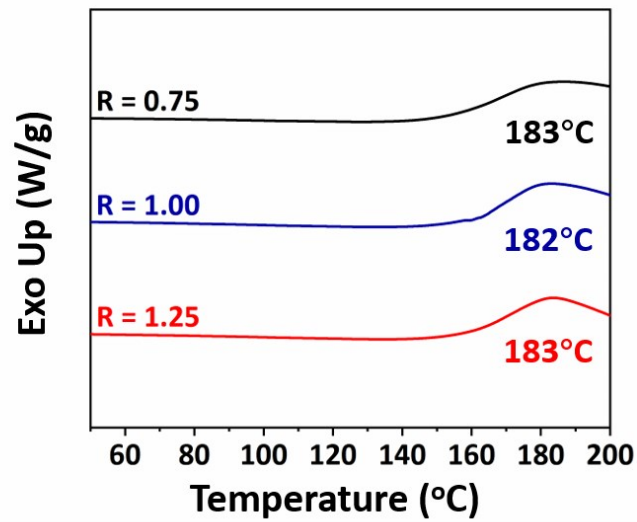


Fig. S2 DSC curves of CPA/ESO without TBD (R = 0.75, 1.00 and 1.25) at a heating rate of 5°C/min.

S3. FTIR spectra of ESO, CPA and CPA/ESO networks

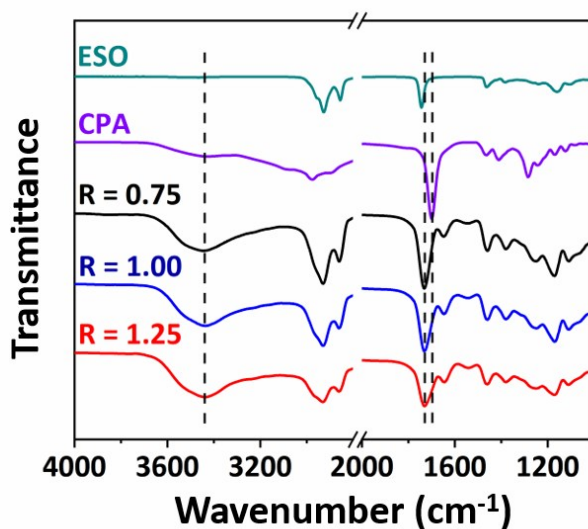
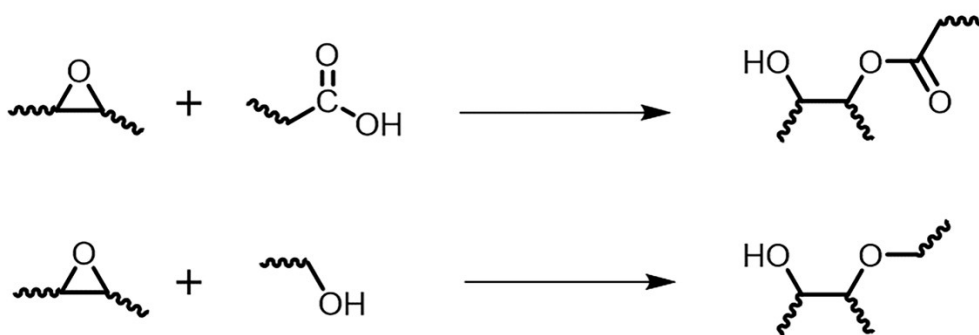


Fig. S3 FTIR spectra of ESO, CPA and CPA/ESO networks (R = 0.75, 1.00 and 1.25, TBD 5 mol %).

S4. Reaction mechanism of ESO with CPA



Scheme S1. Reaction mechanism of ESO with CPA.

S5. DTG of CPA/ESO networks

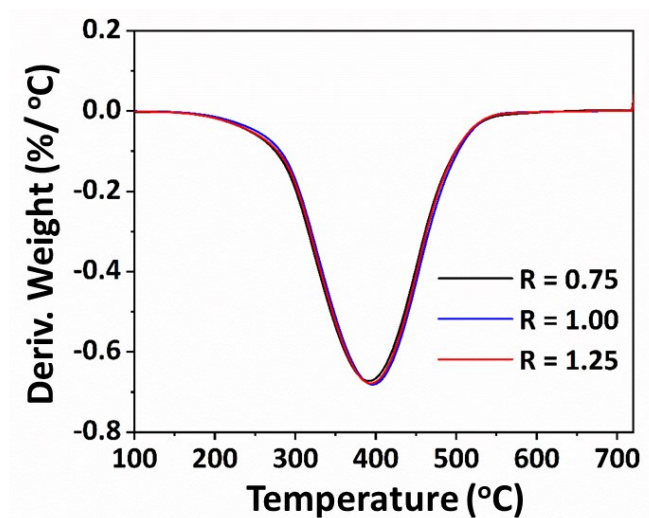


Fig. S4. DTG curves of CPA/ESO networks derived from TGA.

S6. Hydrolysis resistance of CPA/ESO (R = 1.25)

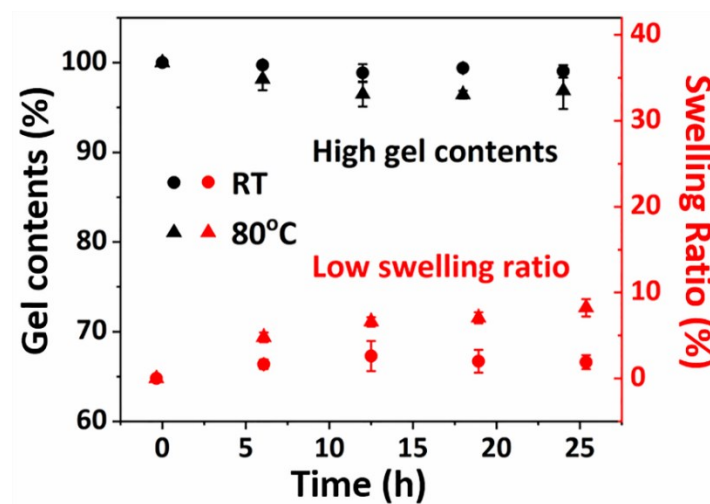


Fig. S5. Gel contents (black) and swelling ratios (red) of CPA/ESO networks (R = 1.25, TBD 5 mol %) in water at room temperature (circles) and 80°C (triangles).

S7. Stress relaxation of CPA/ESO networks

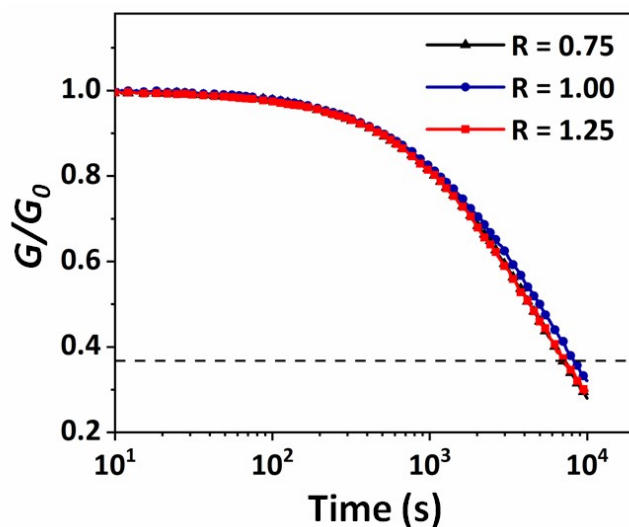


Fig. S6. Normalized shear stress relaxation of CPA/ESO networks ($R = 0.75, 1.00,$ and $1.25,$ TBD 5 mol %) at 200°C .

S8. Calculation of T_v of CPA/ESO ($R = 1.25$)

The T_v of CPA/ESO ($R = 1.25$) was calculated as the following process:

Initially, equation S3 was obtained from Arrhenius law as shown in Fig. 3b:

$$y = 10.055x - 12.34 \quad (r = 0.99) \quad (\text{S3})$$

The Maxwell relation (equation S4) below is used to calculate T_v which is defined as the point at the viscosity $\eta = 10^{12} \text{ Pa S}^{-1}$. The shear modulus G was estimated from tensile modulus (E') as measured by DMA with the relation. E' of the sample was calculated as the average modulus at temperature ranging from 140 to 200°C from the modulus-temperature curves (Fig. 2d). The average plateau modulus of the sample is 0.65 MPa. The Poisson's ratio ν is chosen as the value 0.5, which is usually used for rubbers.

$$\eta = G\tau^* \quad (S4)$$

$$G = \frac{E'}{2(1 + \nu)} \quad (S5)$$

Consequently, $G = 0.65/(2 \times 1.5) = 2.17 \times 10^5$ Pa,

$\tau^* = \eta/G = 1012/(2.17 \times 10^5) = 4.61 \times 10^6$ s,

$\ln \tau^* = \ln (4.61 \times 10^6) = 15.34$.

Using equation S3, $15.34 = 10.055x - 12.34$, $x = 2.75$

Thereby, $1000/T_v = 2.75$, $T_v = 363.64$ K = 90°C .

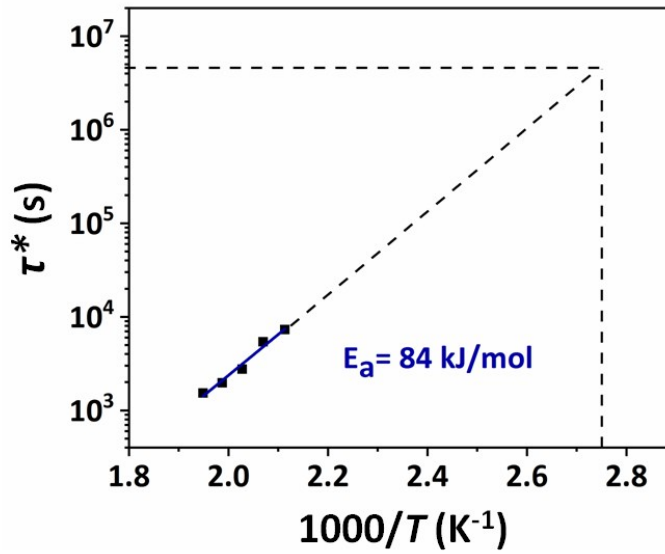


Fig. S7 Topology freezing transition temperature (T_v) calculated by using equation S(3).

S9. Digital photo, flexural tests and DMA of CF/CPA/ESO composites



Fig. S8 Optical photo of the CF/CPA/ESO composite laminates.

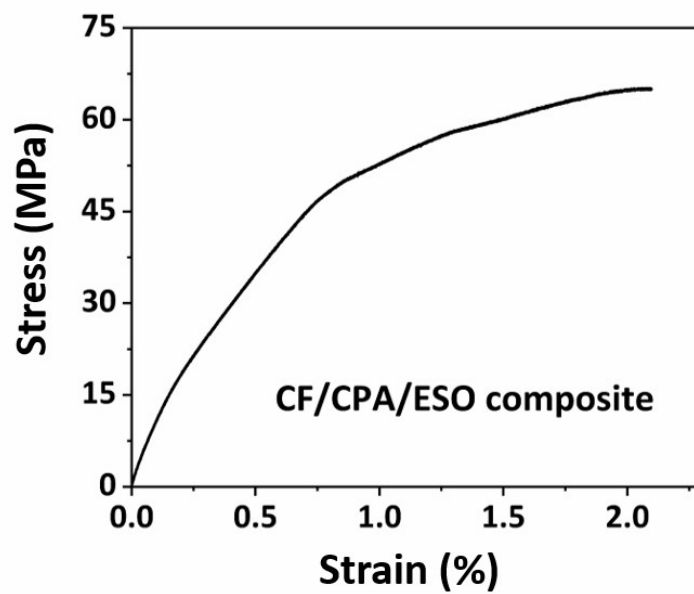


Fig. S9 Flexural tests of the CF/CPA/ESO composite laminates.

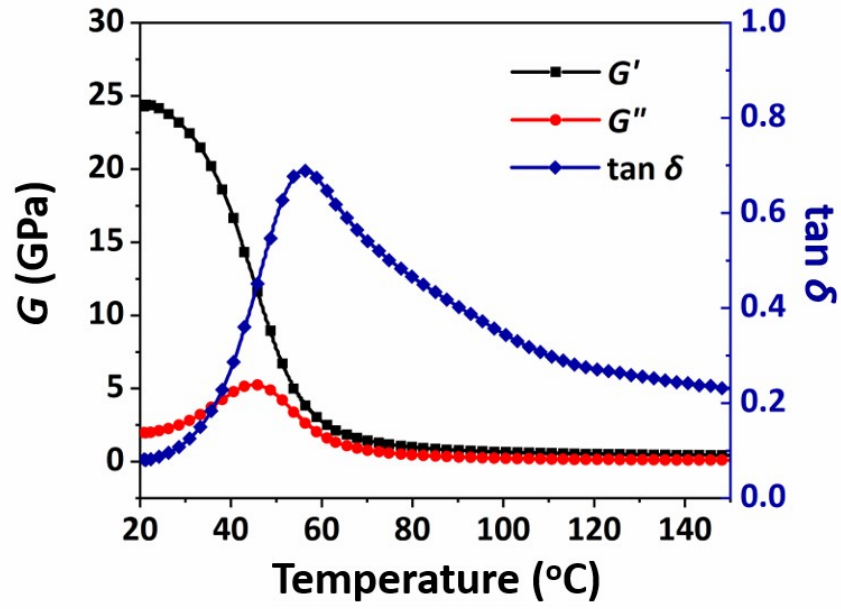


Fig. S10 DMA of the CF/CPA/ESO composite laminates.

S10. Compression performance tests for reprocessed CF/CPA/ESO composite

“M” and CPA/ESO (R = 1.25) matrices.

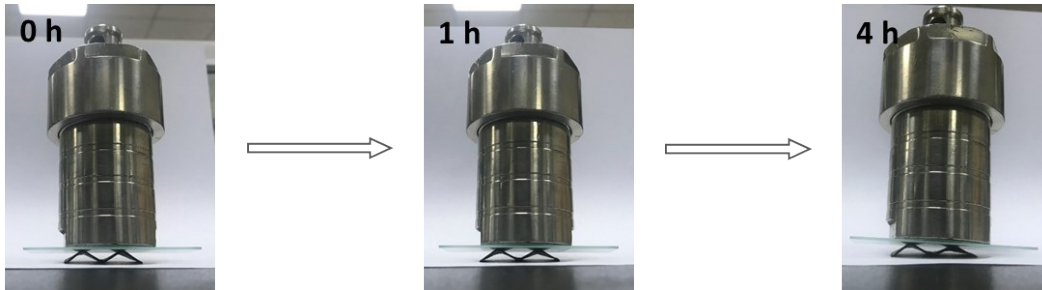


Fig. S11 Digital photos of bearing experiments (1.2 kg weight) for reprocessed CF/CPA/ESO composite “M” at 0 h, 1 h, and 4 h, respectively.

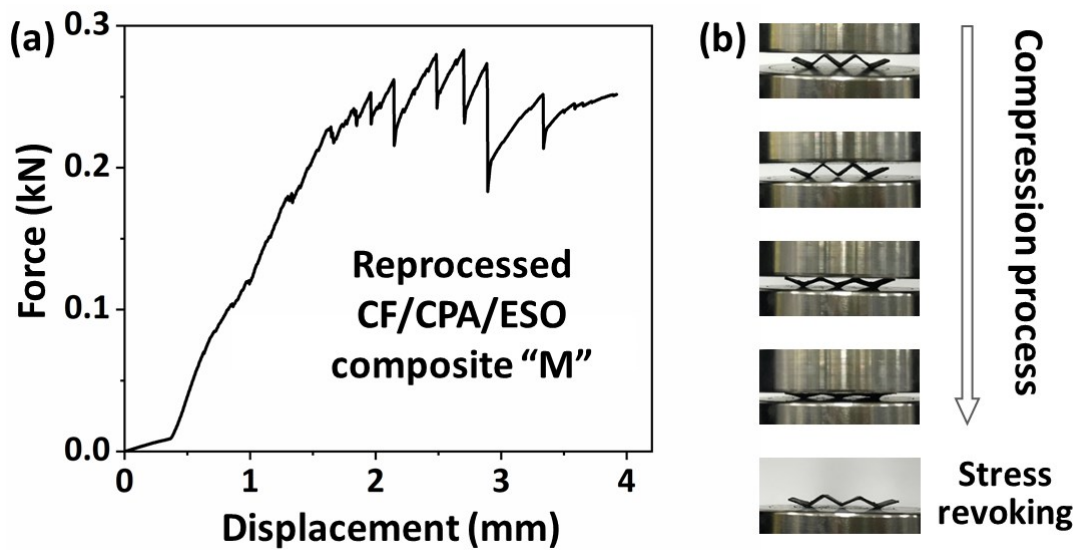


Fig. S12 Compression curve (a) and digital photos (b) of compression process of reprocessed CF/CPA/ESO composite “M”.

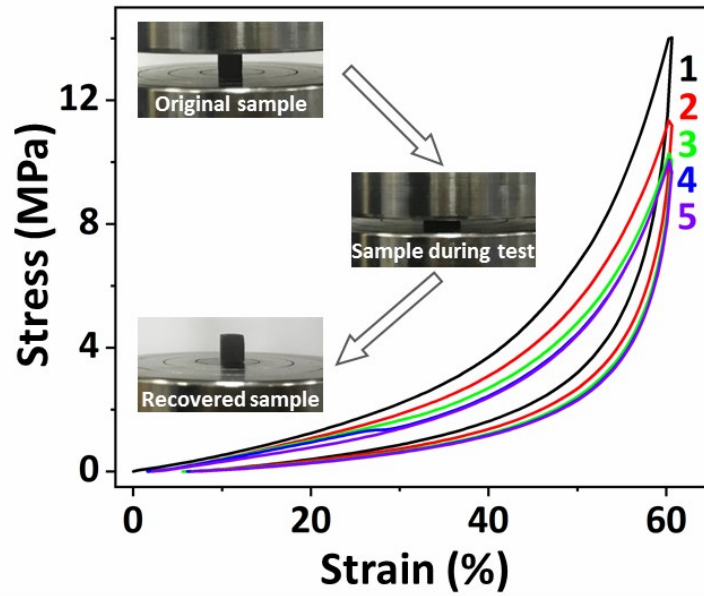


Fig. S13 Stress–strain curves of CPA/ESO ($R = 1.25$) for up to 5 cycles during compression tests. Inset images were the photos of materials before tests, under tests and after tests, respectively.

S11. Repairing properties of CF/CPA/ESO composites at 200°C without EG

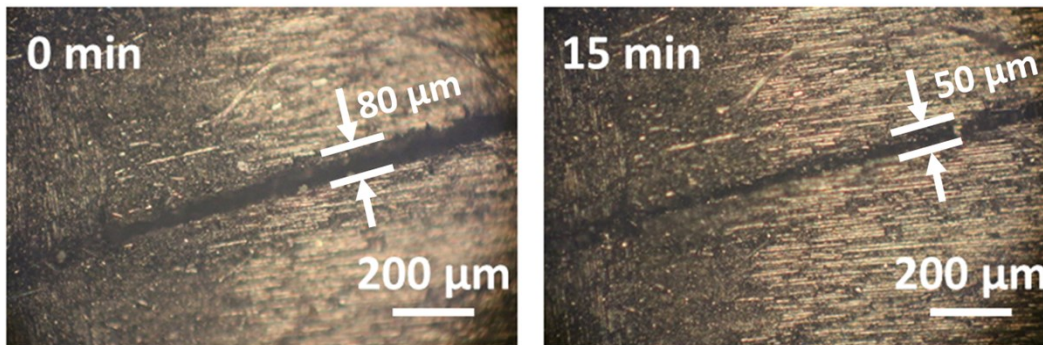


Fig. S14 Optical microscope images of the crack repairing of CF/CPA/ESO composites at 200°C without EG.

S12. Degradation kinetics of pure matrices (CPA/ESO, R = 1.25) in EG at 190°C.

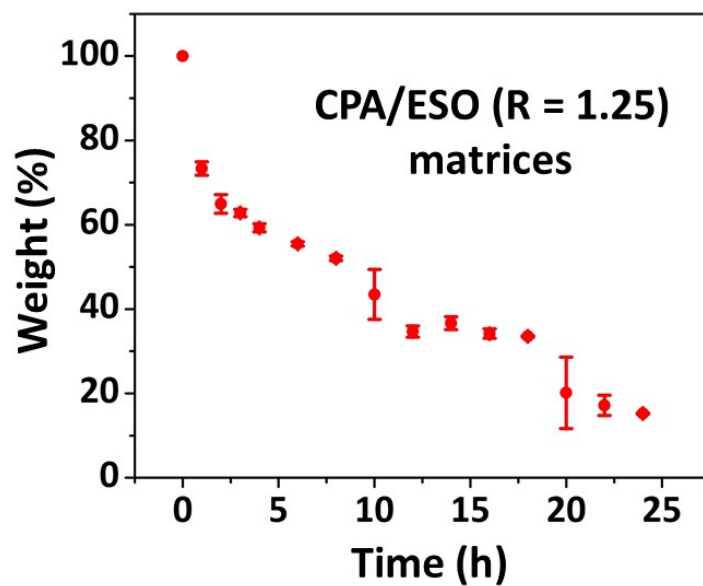


Fig. S15 Degradation kinetics of CPA/ESO (R = 1.25) matrices in EG at 190°C.

S13. Comparison of the matrices in this work with other reported dynamic matrices for fiber reinforced polymers

Table S1. Comparison of the matrices in this work with other reported dynamic matrices for fiber reinforced polymers.

Types of dynamic covalent bonds	Biobased or not	Stress relaxation time (1/e)	pH resistance	Water or solvent resistance	Reference
Schiff base	×	1 s / 80 °C	×	✓	[S1]
Schiff base	✓	30 s / 200 °C	×	✓	[S2]
Spiro diacetal	✓	No mentioned	×	✓	[S3]
Disulfide linkages	×	20 s / 200 °C	✓	✓	[S4]
Vinylogous Urea	×	60 s / 170 °C	✓	×	[S5]
Boronic ester	×	No mentioned	×	×	[S6]
Ester bonds	×	660 s / 200 °C	✓	✓	[S7]
Ester bonds	×	660 s / 200 °C	✓	✓	[S8]
Ester bonds	×	600 s / 210 °C	✓	✓	[S9]
Ester bonds	✓	7245 s / 200 °C	✓	✓	This work

References

- [S1] P. Taynton, H. Ni, C. Zhu, K. Yu, S. Loob, Y. Jin, H. J. Qi and W. Zhang, *Adv. Mater.*, 2016, **28**, 2904-2909.
- [S2] S. Wang, S. Ma, Q. Li, X. Xu, B. Wang, W. Yuan, S. Zhou, S. You and J. Zhu, *Green Chem.*, 2019, **21**, 1484-1487.
- [S3] S. Ma, J. Wei, Z. Jia, T. Yu, W. Yuan, Q. Li, S. Wang, S. You, R. Liu and J. Zhu, *J. Mater. Chem. A*, 2019, **7**, 1233-1243.
- [S4] A. R. Luzuriaga, R. Martin, N. Markaide, A. Rekondo, G. Cabanero, J. Rodriguez and I. Odriozola, *Mater. Horiz.*, 2016, **3**, 241-247.
- [S5] W. Denissen, I. De Baere, W. Van Paepegem, L. Leibler, J. Winne and F. E. Du Prez, *Macromolecules*, 2018, **51**, 2054-2064.
- [S6] S. Wang, X. Xing, X. Zhang, X. Wang and X. Jing, *J. Mater. Chem. A*, 2018, **6**, 10868-10878.
- [S7] K. Yu, Q. Shi, M. L. Dunn, T. Wang and H. J. Qi, *Adv. Funct. Mater.*, 2016, **26**, 6098-6106.
- [S8] L. Yu, C. Zhu, X. Sun, J. Salter, H. Wu, Y. Jin, W. Zhang and Rong Long, *ACS Appl. Polym. Mater.*, 2019, **1**, 2535-2542.
- [S9] Erwan Chabert, J. Vial, J.-P. Cauchois, M. Mihalutac and F. Tournilhac, *Soft Matter*, 2016, **12**, 4838-4845.